Proceedings of the 32th International Conference on Ocean, Offshore and Arctic Engineering
OMAE2013
June 9-14, 2013, Nantes, France

OMAE2013-11356

WAVE MODELLING FOR POTENTIAL WAVE ENERGY SITES AROUND THE OUTER HEBRIDES

Charles E Greenwood
Lews Castle College, University of the Highlands and Islands
Stornoway, Isle of Lewis, Scotland

Vengatesan Venugopal
University of Edinburgh
Edinburgh, Scotland

David Christie
Lews Castle College, University of the Highlands and Islands
Stornoway, Isle of Lewis, Scotland

James Morrison
Lews Castle College, University of the Highlands and Islands
Stornoway, Isle of Lewis, Scotland

Arne Vögler
Lews Castle College, University of the Highlands and Islands
Stornoway, Isle of Lewis, Scotland

ABSTRACT

This paper presents the results of a numerical wave modelling study carried out to assess the near shore wave energy resource around potential wave energy sites at the Outer Hebrides in the United Kingdom. This study uses Danish Hydraulic Institute's MIKE 21 Spectral Wave model suite. Input boundary conditions are obtained from a Datawell directional wave buoy located approximately 16 km off the coast of Lewis in 60 metre depth. Additional data collected from a submerged Acoustic Wave and Current profiler (AWAC) located at 13 metre depth offshore at one of the wave energy development sites was used to calibrate and validate the wave model for separate time periods. The calibration process allows the manipulation of white capping, bottom friction and wave breaking parameters to alter the energy dissipation across the model domain. The altered parameters gave a significantly better agreement between modelled and measured results than the model defaults. While the average wave conditions provided a relatively straightforward calibration process the more extreme storm events significantly under predicted the wave height. After several trials in altering model coefficients a good agreement was reached between the model results and the AWAC data. These new sets of calibration parameters enable the simulation of wave heights within 13% for the AWAC data and marginally more for wave periods for the first 6 months of 2012.

1. INTRODUCTION

With increasing global energy demand and concerns about anthropogenic climate change world governments are under increasing pressure to find alternative forms of energy. The development of extracting carbon neutral energy has undergone radical changes in recent years, where technologies such as wind and solar power have accelerated to become commercially viable power sources. Other renewable technologies are now being developed to ensure a diverse and reliable energy mix. The Scottish government has set a target of producing 100% of its electrical energy demand by renewable means by 2020 [1]. Advancements in the wave energy industry will soon allow the deployment of large scale arrays capable of producing multiple megawatts (MW). This has led to large scale development plans for the wave industry off the west and north coast of Scotland. The west coast of the Isle of Lewis (Outer Hebrides) has been identified as an area of high wave energy density and has attracted the interest of several commercial developers. Aquamarine Power have successfully gained two lease sites on Lewis and plan to extract up to 40MW [2], Pelamis Wave Power have been granted a lease for a 10MW array [3] and Voith Hydro Wavegen has submitted plans to construct a 1.2km breakwater that will extract 30MW, although this latter development has currently been shelved due to a lack of investment and electrical infrastructure [4]. The overall results of these deployments will see a cumulative energy production of up to 80MW. The location of these sites is shown in Figure 1. With growing interest in the west coast of the Hebrides from wave energy developers the spatial distribution of wave energy is of great importance for current and future wave energy developments.

This study focuses on applying Mike 21 SW (Spectral Wave) model developed by DHI (Danish Hydraulic Institute) [5] for the assessment of the transformation of waves in coastal waters around the Isle of Lewis in the Outer Hebrides. Existing wave resource information for the Outer Hebrides is obtained from national scale, seasonally averaged maps. The Atlas of

Copyright © 2013 by ASME

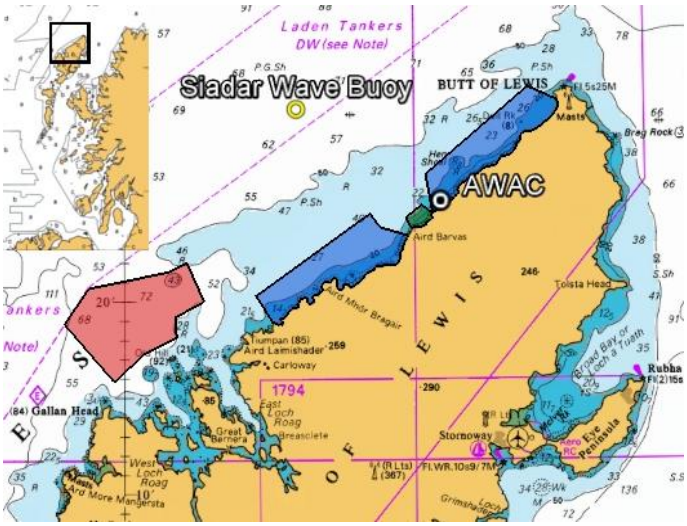

Figure 1. Study area showing WEC development sites (West to East Pelamis wave Power, Aquamarine Power 1, Voith Hydro Wavegen, and Aquamarine Power 2) and wave data sensors.

UK Marine Renewable Energy Resource [6] was developed in order to aid the industry on the identification of high energy resource sites around the UK. The model provides seasonal wave height averages within the domain and indicates that the west coast of the Outer Hebrides has some of the largest wave heights in the UK. Due to the large scale of the domain the model resolution is coarse. While this model does provide a reasonable assessment of the UK's average wave height, this model is unsuitable for quantifying the available resource distribution for specific proposed wave energy sites to the spatial and temporal resolution required by developers. More recent studies that look at the UK distribution of wave energy as opposed to wave height also exhibit similar spatial resolution and time averaging limitations [7, 8]. The results of these studies support the general wave energy distribution shown in the discussed studies, where the Outer Hebrides receives the largest wave resource in the UK.

More detailed wave resource models for WEC (wave energy converter) sites are not generally released into the public domain due to commercial sensitivities. However there are some available academic studies of the environmental impacts of WEC arrays available. These models focus on comparing the pre- and post- installation wave climates [9, 10]. The very nature of comparing the alteration of the climate around devices requires these models to be of a fine scale. Within this process the deployment site is already identified and the aim is to determine the alteration to the wave climate and the near shore affects.

As further research into the environmental impact of WEC arrays advances, quantifying the initial resource by using finer scale maps will be essential. While this does provide advancements in mapping the initial resource, the fine scale nature of the domain limits the use of these studies for potential site identification. This has left a gap for a broad-scale approach where the regional resource distribution is assessed. This mid-scale model resolution will allow the assessment of multiple potential sites within a single model domain. Further benefits allow a more detailed spatial and temporal resolution than the national scale model while including other potential sites within the region.

For the present work the Mike 21 Spectral Wave (SW) model is chosen due to its suitability for both deep and shallow water domains with finer scale grid spacing. The model simulates the build-up and transformation of wind and swell waves in the offshore and near shore environments. The SW software consists of two independent wave models, the fully spectral formulation and the directional decoupled parametric formulation. This study only considers the fully spectral formulation, which is based on using the wave action conservation equation to track the evolution of directional frequency spectra. This allows the model to account for bathymetric refraction and shoaling, wave induced currents, and tidal variations, while wind forcing, nonlinear wave interactions, white capping, bottom friction and depth induced breaking are included as source terms. By using a cell-centred finite volume-technique the model applies an unstructured mesh grid to propagate the wave action through the model domain using phase averaged equations. Further details on the SW model can be found in the user manual [5]. The methodology used for the wave modelling, calibration, validation and results obtained are detailed in the following sections. Considering the space limitations, detailed discussions for wave power are made in this article.

2. METHODOLOGY

This study applies the Mike 21 SW model to the west coast of the Isle of Lewis in order to assess the spatial and temporal distribution of wave energy. The model domain was identified by including some of the potential development sites shown in Figure 1. Multiple sources of bathymetry data were used, these are further outlined in section 2.1. The model boundary conditions were driven using time varying wave spectra from the Siadar directional wave buoy. Further wave data was collected from a submerged AWAC (Acoustic Wave and Current profiler) and used to calibrate and validate the wave model.

2.1. Computational Domain

The computational domain for this assessment focuses on the nearshore locations leased to Voith Hydro Wavegen and Aquamarine Power (ref to Figure 1). The default bathymetry data used for this study consists of the GEBCO 08 data [11]. GEBCO 08 is an open-source global bathymetry data set with a resolution of 30 arc seconds. This dataset was created using interpolated depth sounding and satellite gravity data. The choice of modelling site enabled this relatively coarse data to be supplemented in the region between the 60m and 20m contours with a high-resolution open-source data created by Marine Scotland for the north-west coast of Lewis. To match the model resolution this $3m^2$ data was filtered to $20m^2$. A

Copyright © 2013 by ASME

further dataset was collected by Aquamarine Power that covers the shallow waters behind their potential development site. This data extending from 5m to -15m with a resolution of less than $1m^2$, (again filtered to $20m^2$ resolution). All bathymetry datasets discussed above were converted to the UTM-29 coordinate systems and to chart datum water levels.

The unstructured domain mesh uses separate mesh resolution steps that increase in detail towards the area of interest around the development sites (where the elements are approximately 100m apart), with less important and deeper areas covered by a coarser grid to conserve processor power. The domain was lengthened by adding a coarse section to the south west, so that the model, when driven from the north-western boundary, could more accurately handle the incoming waves, as explained in the next section. The final mesh, shown in Figure 2, has 2011 elements.

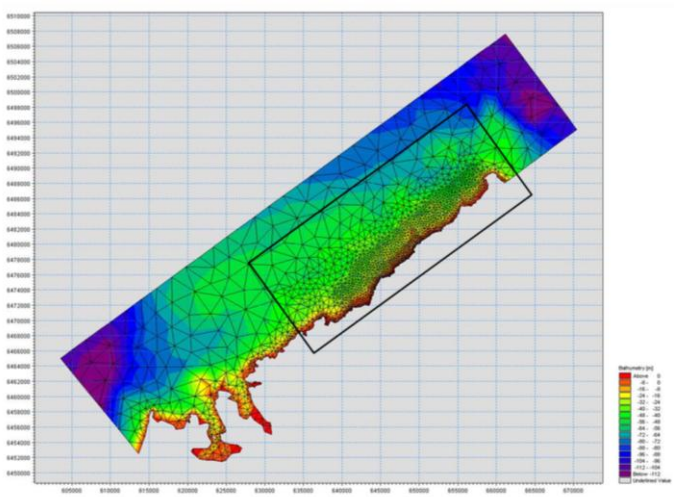

Figure 2. Nested computational domain where warmer colours indicate shallower water depths with the area of interest depicted within the rectangle.

2.2. Boundary Input Parameters

The boundary conditions are driven by a Datawell MK III directional wave buoy (marked Siadar wave buoy) deployed in 60m depth at the location shown in Figure 1. The MK III wave buoy provides directional wave spectral information, x, y and z displacements and a magnetic compass [12]. The time series displacements are sampled at 1.28Hz for a 200 second period where an FFT (Fast Fourier Transformation) is used to create a frequency spectrum. The Datawell software combines 8 of these spectra to create a 30 minute spectral file, using an additional 200 seconds for calculations and storage. The resulting spectral file consists of 64 frequency bins ranging from 0.025Hz to 0.58Hz and their associated Power Spectral Densities (PSD). Directional information is encoded in the peak direction, spread, skew, and kurtosis for each frequency bin, which come from the first two Fourier components of the directional spreading function. A directional frequency spectrum is created combining the energy frequency distribution *E(f)* (which is the same as the PSD), and directional spreading function *D(f,θ)* to give a directional spectral density *E(f,θ)*:

$$E(f,\theta) = E(f)D(f,\theta) \tag{1}$$

As the wave buoy only produces *E(f)* in the spectral file the directional component must be generated from a calculated directional distribution using the wave buoy given directional parameters. One of the simplest forms of directional distributions uses a normal or Gaussian distribution across *E(f)* and can be shown as

$$D(f,\theta) = \frac{exp\left[-\frac{1}{2}\left(\frac{\theta-\theta(f)}{\sigma}\right)^2\right]}{\sqrt{2\pi}\,.\,\sigma} \tag{2}$$

Here, θ represents peak direction, $\theta(f)$ is the wave component direction with frequency 'f' and σ is the wave spread. All directions including spreading should be calculated in radians for later use. To ensure the directional spectrum is compatible with Mike 21 SW the data must be filtered in the frequency domain to a linearly spaced distribution. This removes some of the lower frequency values resulting in 56 frequency bins ranging from 0.03-0.58Hz with a 0.01Hz spacing. For this study the spectral discretisation within the model will be run for 56 frequencies

The wave conditions were measured continuously for a year period from 1st December 2011 to the 30th November 2012, providing 17571 data points at the model boundary. To achieve this unbroken dataset any gaps in the recorded wave conditions were interpolated across, providing mock data files for the missing data. The number and the time location of the mock files were logged providing a total of 545 missing files for the year period. To effectively replicate the existing wave conditions within the domain the characteristics and likely wave parameter of the local wave climate should be identified. Figure 3 shows a wave power rose for a year's data, this shows mean wave direction and percentage power plotted in 10° bins. Wave power was calculated using wave buoy parameters and linear wave theory, where the location of the wave buoy is assumed to be deep water. It can be seen that the majority of waves propagate from 290° with a secondary peak originating from 30°. This level of variation in the incoming swell provides some challenges regarding the orientation of the main driving boundary. Due to the two peak wave direction observed in Figure 3, the North West boundary of the model domain is angled parallel to the shoreline and extended beyond the area of interest. This allows the propagation of waves through to the area of interest without experiencing interference from the other boundaries. The presence of the two peaks may potentially indicate the presence of bi-modal seas. With the focus of this study on identifying and quantifying the potential resource for the west coast of the Isle of Lewis the inclusions of bi-modal sea is likely to cause a significant impact on the results. This observation supports use of a fully directional

Copyright © 2013 by ASME

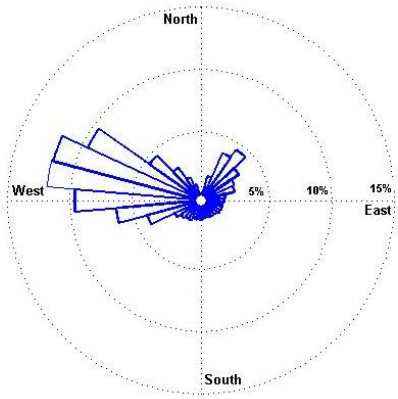

Figure 3. Mean directional wave power rose.

frequency spectrum generated from measured data as model boundary conditions. Figure 4 shows a time series of the measured wave heights together with the weekly average. The duration of the measurements enables the observation of the seasonal change in wave height and the weekly averages. When the 30 minute and weekly averages are compared the winter months show a high level of variation around the weekly average in contrast with the summer.

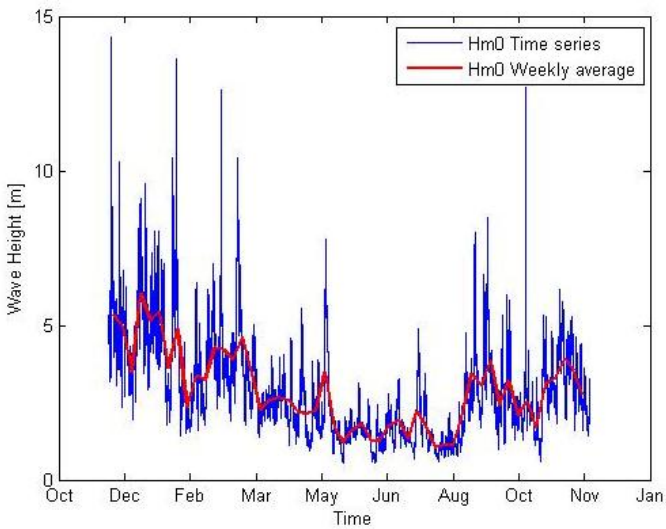

Figure 4 Time series of wave height for the 2011/2012 period.

When wave height and period are considered (see Table 1) and compared to a similar scatter table as exhibited in Smith et al [10] for the Wave hub site, it can be seen that there are some differences in the annual wave climates. While the datasets from the present study and Smith et al [10] do not cover the same time frame or region, a reasonable comparison can be drawn. When compared in the frequency domain the Hebridean wave buoy measured a higher occurrence of lower frequency waves with lower peak values. The level of variation recorded across the frequency domain was significantly higher for the Hebridean wave buoy than the one at the Wave hub location. When wave heights are considered the Hebridean wave buoy recorded a larger percentage of data points with significantly higher wave heights than the Wave Hub. The combination of lower wave frequencies (i.e. longer waves) and higher wave heights make the Isle of Lewis an attractive place for WEC array deployment; however the larger variation in wave conditions means WEC technologies need to be well proven and have more complex device tuning systems to efficiently extract the larger resource. The increased variation in wave climate requires a more complex model that can account for large sudden changes in wave height and period along with the presence of bi-model sea states.

Table 1. Parameterized sea state and percentage of occurrence

Hm0 \ Tz	3	4	5	6	7	8	9	10	11	12	13
12										0.02	0.01
11									0.02	0.01	
10							0.01	0.05	0.03	0.05	0.03
9							0.05	0.10	0.13	0.09	
8						0.01	0.21	0.43	0.22	0.12	
7						0.13	0.79	0.75	0.24	0.02	0.01
6					0.05	0.92	1.85	0.96	0.14	0.05	
5				0.08	0.77	3.02	2.78	0.67	0.19	0.03	
4			0.01	1.09	4.93	5.46	2.08	0.43	0.14	0.05	
3			1.58	5.73	7.29	4.27	1.69	0.36	0.13	0.01	
2	0.01	2.33	8.02	10.66	6.68	2.49	0.69	0.08	0.03		
1	0.73	4.68	8.26	3.66	1.23	0.13	0.03	0.03			

The model is solely driven by the north-west boundary. The majority of waves approach between (just under) 270 and 360 degrees. Extending the length of the boundary allows waves from this range of directions to propagate to the area of interest without being significantly affected by the remaining closed boundaries.

As the area of interest, AWAC and potential development sites are situated in shallow water the variation in water depth caused by tidal constituents must be included. As the area of coast is relatively simple with regards to the generation of tidal currents only the variation in water depth across the domain is considered. The tidal data was extracted from the DHI Global Tidal Model. This model calculates the tidal variation based on the first 8 tidal constituents on a global scale with a resolution of 0.25°.While DHI advise against using this data for regions of water depths below 20m it provides a reasonable agreement with measurements taken from the AWAC for the corresponding time period. A comparison between the AWAC and the global tidal model can be seen in Figure 5 where the phase and amplitude of the modelled data agrees with that of the measured data. This provides a reasonable representation of water depths for the entire model time period.

2.3. Model Setup

Within the fully spectral formulation in Mike21 SW, several parameters can be adjusted to define the type of model which will be run. This section briefly describes the model setup for resource assessment for WEC arrays. The model time step was set as an hourly interval. This level of detail will provide a more accurate account of storm conditions where the rate of energy transfer is high, as opposed to a more standard 6 hourly time step. The time formulation used is a quasi-stationary formula that calculates a solution for each time step

Copyright © 2013 by ASME

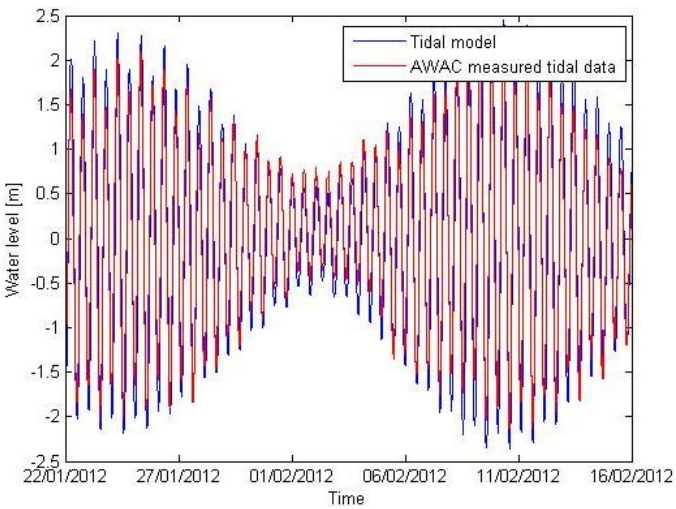

Figure 5. Comparison between AWAC measured tide and DHI Global tidal model for a spring neap cycle.

providing a time series dataset. The spectral discretization used for the formulations within the model was defined for frequency as 56 bins ranging from 0.03 to 0.58Hz at a 0.01Hz interval similar to that of the boundary conditions. The directional discretization defined using 36 bins resulting in a 10 degree resolution. The solution technique used within the model used the default low order fast algorithm and a modified version of the Newton Raphson iteration equation. The tolerances within the model were made less stringent, the number of iterations remained as the default values, where the tolerances for the Root-Mean-Square (RMS) norm of a residual vector and the max-norm of the significant wave height where altered to $1x10^{-6}$ and 0.1 respectively.

3. MODEL CALIBRATION

The calibration process within Mike21 SW utilizes additional model parameters based on energy dissipation terms. These parameters can be used as calibration terms. They include; wave breaking, which controls dissipation through depth induced breaking; bottom friction, which controls propagating waves orbital velocity interaction with the seabed; and white capping, which controls energy dissipation through wave steepness. The process of calibrating a model to correlate with existing wave data is an iterative process that is done over a series of model simulations.

In order to calibrate the wave model the data measured by the AWAC was used. The device was deployed in 16m depth of the north-west coast of the Isle of Lewis (shown in Figure 1) on the 17th of January 2012. This device uses a combination of acoustic and pressure sensors to measure waves. As this device requires manual data collection at the date of this study only 6 months of data had been collected. The AWAC data allows a comparison between the measured data and model output for the same location. By assessing the difference between the measured and modelled wave parameters a more accurate calibration process can be performed using simple statistical analysis to calculate the Bias, RMS Error, and the Scatter index shown below.

$$Bias = \frac{1}{N}\sum_{i=1}^{N}(x_i - y_i)^2 \tag{3}$$

$$RMS\ error = \sqrt{\frac{1}{N}\sum_{i=1}^{N}(x_i - y_i)^2} \tag{4}$$

$$Scatter\ Index = \frac{RMS\ error}{\bar{x}} \tag{5}$$

Here, N is the number of samples, x_i is measured dataset, y_i is the modelled dataset and $\bar{x}$ is the mean of the measured dataset.

Due to the high-resolution of wave data across the model and the computational time requirements, model calibration was conducted for a shorter time period, during the winter months where AWAC data is available. By using a relatively small time series from the winter period the seasonal variation can be accounted for. This time series was identified within March 2012 as it contains some of the larger recorded wave heights from the AWAC.

For calibrating the wave model the first stage of the calibration process uses the white capping parameter. This source term uses two parameters within an equation developed by Hasselman [13]. The main displacement coefficient (C_{ds}) that controls the magnitude of energy dissipation and a second frequency based term (δ) alters the energy dissipation across the frequency domain. As this term quantifies losses through wave steepness and breaking the effectiveness of this term are suited to calibrating larger scale models. If white capping is used to significantly increase energy loss within a small domain the value may extend beyond realistic values providing unreliable data. For relatively small domains, where energy loss from white capping is negligible, the main calibration parameter is bottom friction. This process changes the bottom friction parameters in an attempt to alter energy dissipation. The bottom friction source term is based on the equation by Battjes and Janssen [14]. Within the SW model the sea bed interaction can be applied in several forms, this study uses the Nikuradse roughness (*kn*). The default parameter for the Nikuradse roughness is 0.08m. Figure 6 shows the effects of altering these parameters on the wave height over a short time frame form 2nd to the 13th of March 2012. The default *kn* value of 0.04m simulates a higher wave height for the duration of the simulation. By increasing the bottom friction, the rate of energy dissipation across the model is increased, reducing the wave height at the AWAC location. This is shown in Figure 6 where the red dotted line more accurately represents the measured data.

Copyright © 2013 by ASME

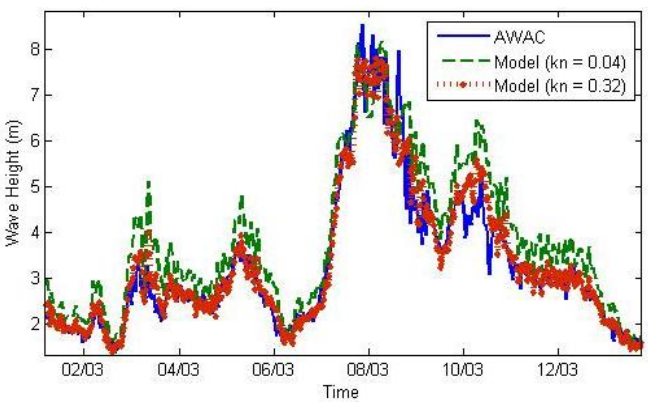

Figure 6. A direct comparison between measured and modelled wave height data where bottom friction has been altered.

This qualitative method for assessing the relationship between measured and modelled data is limited. For the more fine scale calibrations, statistical analysis is implemented. When the statistical parameters are calculated for the default value of bottom friction the model shows a bias of 0.50, RMS error of 0.70 and a scatter index of 0.22. When bottom friction is increased from the default to 0.32, the simulated wave height is shown to have a better agreement with a bias of 0.03, RMS error of 0.34 and a scatter index of 0.11. This higher bottom friction value was then applied to the entire duration of the AWAC dataset where the model can be calibrated for seasonal variations in a more controlled approach. Figure 7 shows the model agreement between a parameter based models with the AWAC data with regards to bottom friction. A quadratic fit was applied to the data, this suggests that optimal bottom friction value is between 0.3 and 0.35. As the bottom friction value approaches the optimum value the rate of change in the scatter index is reduced. To get the optimal model calibration coefficients the model runs a finite number of times. However, due to computational time limitations a compromise is made, where a value within an acceptable error tolerance is taken and applied for the duration of the model. While the results for Figure 7 were based on a parameters based model the calibration values from this graph were taken and applied to the directional frequency spectra model.

Further model calibrations focus on the alteration of energy dissipation across the frequency spectra. This requires the manipulation of the δ coefficient within the white capping parameter using the same technique used for adjusting the wave height. Figure 8 shows the agreement between AWAC and simulated data when the energy dissipation across the frequency is changed for the same time period as Figure 6. Due to the large storm event that occurred around the 8th of March 2012 the recorded wave period data contained large amounts of potential errors and was therefore removed. Figure 8 shows the simulated output for δ = 0.5 significantly over predicting the mean wave period, when δ is reduced to δ = 0.001 a better agreement between the measured data and the model output can be seen. Figure 8 shows the simulated output for δ = 0.5

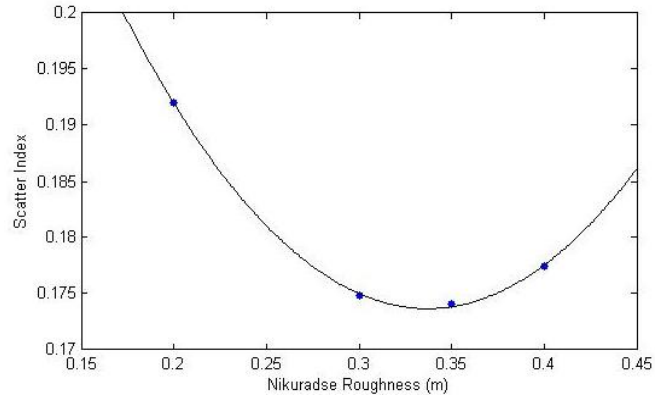

Figure 7. Model Scatter index with regards to Nikuradse roughness

significantly over predicting the mean wave period, when δ is reduced to δ = 0.001 a better agreement between the measured data and the model output can be seen. When the statistical method is applied to the data shown in Figure 8 a δ coefficient equal to 0.5 has a bias of 1.53, RMS error of 1.73 and a scatter index of 0.218. As the δ coefficient is reduced to 0.001 the bias, RMS error and scatter index becomes 1.53, 1.12 and 0.17 respectively, resulting in a more accurate simulation of mean wave period.

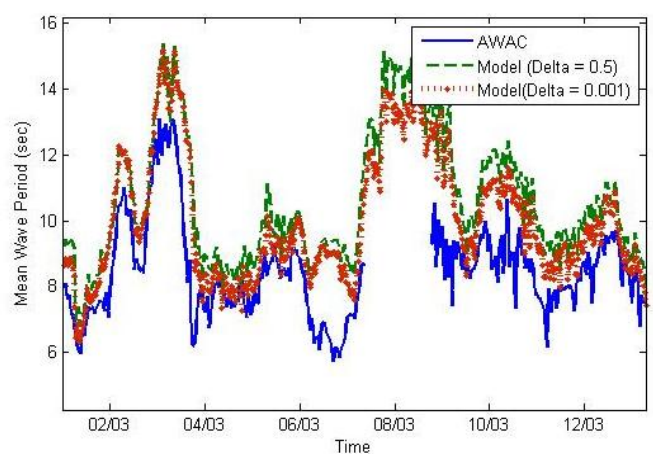

Figure 8. A direct comparison of model and measured data with regards to varying δ dissipation.

When the statistical data is compared with other literature the values for RMS error and scatter index can be put into prospective. A study verifying third generation wave model for coastal regions achieved an average RMS error value of 10% wave height and period [15]. When this is compared with the calibration results, the data shows a RMS error value of 11% of the mean significant wave height and 14% for the mean wave period. However when the scatter index is compared to the existing research the previous accepted scatter index for significant wave height was recorded at 0.37 and 0.2 for the mean wave period. This shows a dramatic reduction in the scatter index for the present model when considering wave

Copyright © 2013 by ASME

height and small reduction for wave period for the calibration period.

4. RESULTS AND DISCUSSION

Mike21 SW model provides several outputs. To enable a simple comparison the results are compared using wave parameters. As the driving boundary input uses directional frequency spectra the effects of bimodal sea states can be included within the model results analysis. The output parameters covered in the Mike21 SW model allow for the production of a time varying area plot, single point wave parameters and single point directional frequency wave spectra. Single point time series evaluated at the AWAC location enable comparison to be made with the sensor data over the six month period covered by the measurements. For example, Figure 9 shows wave height variation for the entire model and measured datasets. The highlighted grey segment indicates the period of calibration for the model, allowing the remaining AWAC data to be used for validation purposes. The wave height correlation is calculated for the extent of the measured data the statistical bias = -0.05, the RMS error = 0.25 and the scatter index = 0.13. This allows the model to predict wave height within 13% for the AWAC location, which is considered a good agreement. When the variance coefficient is calculated for the mean wave period and peak-wave period a scatter index of 0.14 and 0.07 respectively can be seen.

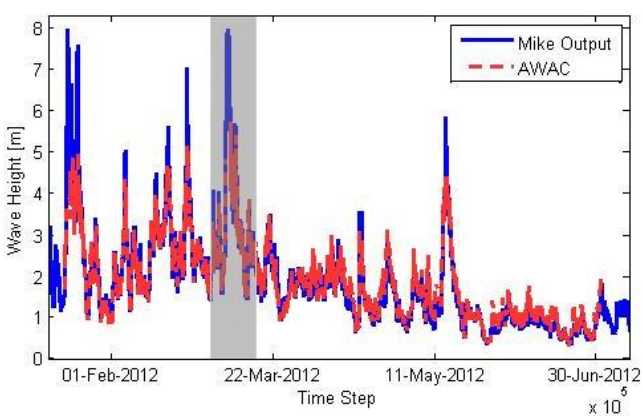

Figure 9 Time series of model and measured wave height with calibration period highlighted in grey.

For the most part the simulated results provide a good indication of the recorded wave parameters at the AWAC site. If the 0.07 scatter index agreement between the measured peak wave period and modelled output is considered, the low scatter index may be attributed to the high occurrence of dominant long period swell. Whereas the statistical result suggest a slightly higher scatter index for the mean wave period, this may be caused by the lack of wind data as the modelled waves propagate across the model domain.

While the model is calibrated temporally to a single point in the model domain the distribution of wave energy can be assessed using spatial model outputs. To assess the spatial distribution of wave energy the results are presented in a time averaged format. While sacrificing temporal variation, this representation allows an insight into the energy distribution on the north-west coast of Lewis. Figure 10 shows the results of the year long simulation calibrated using the March 2012 wave data. The coarse outer regions of the model domain have been excluded to allow a more detailed look at the area of interest, the extent of the domain of Figure 10 is shown with the highlighted rectangle of Figure 2. A series of data points shown in Figure 10 follows the 10m depth contour at 100m spacing. The results show a reduction in wave power as the waves propagate to shallower waters. Further variations in power along the coast can be seen around headlands and inlets. Regions of increased power are shown to be located in areas of exposed outcrops and regions of reduced power are located in sheltered inlets. This spatial variation in average power is caused by bathymetric variations resulting in wave refraction.

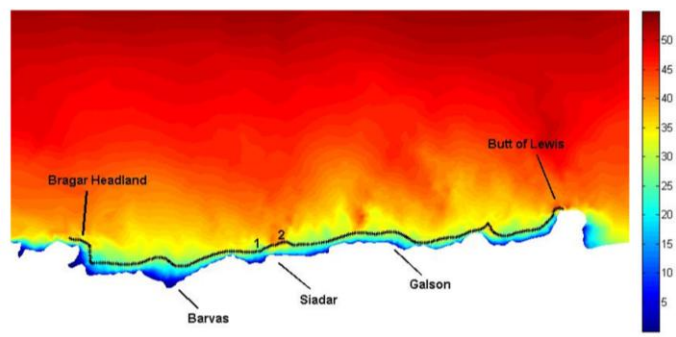

Figure 10 Average distribution of wave power in KW/m for the North West coast of Lewis.

The two locations shown within Figure 10 near Siadar (marked as site 1 and 2) indicate the locations of the initial planned stage for the WEC development for two separate developments. Figure 11 shows the average spatial wave power distribution in detail around sites 1 and 2. The distribution of average wave power along the coast provides important data for the positioning of these WEC arrays. The modelled data shows that site 1 has a lower average wave power than site 2. When the average wave power at the 10m contour is plotted a more detailed analysis of the shoreline resource can be undertaken. Figure12 shows the average wave power from the data points presented in Figure 10 along the Easterly coordinate. Reference locations from Figure 10 are shown in Figure 12 as grey shaded regions. The observed relationship between maxima and minima around headlands and inlets in Figure 10 is also shown in Figure 11 and 12. The time averaged results suggest a 22KW/m variation across the coastline with the peak resource being situated at the Butt of Lewis. Siadar is located within the second highest level of resource, where sites 1 and 2 can be seen in Figure 12 as 646200m and 647500m east (UTM 29) respectively. When a direct comparison between sites 1 and 2 is conducted, site 1 is shown to receive an average wave power of 25.03kW/m while site 2 experiences a more energetic 28.96kW/m. When compared, the results suggest that the

Copyright © 2013 by ASME

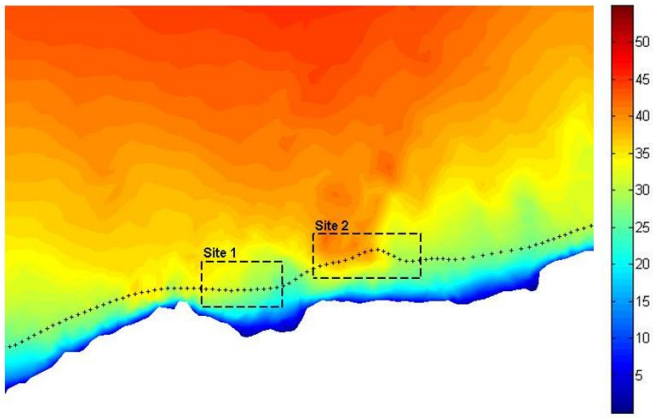

Figure 11 Spatial wave power distribution around sites 1 and 2 in kW/m.

lower resource at site 1 may not offer the optimum positioning for a hypothetical WEC array. Nevertheless the average level of resource for both sites is deemed to be high and other locational benefits may be taken into account such as sea bed type and existing local infrastructure in positioning of arrays.

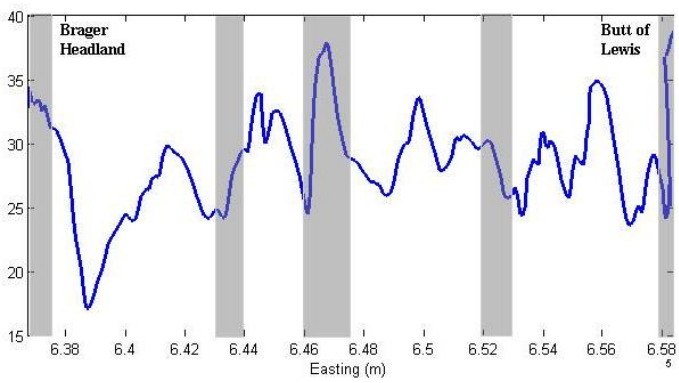

Figure 12 Average wave power across the 10m depth contour in KW/m.

The model does not account for all environmental processes, including reflections. The shallow near shore nature of the AWAC and potential WEC array locations means that there will be some reflection from the shoreline, therefore there will be some variation in the simulated wave spectra from the measured wave spectra. However, the comparison of the AWAC and model data shows a good agreement indicating that while the model does not account for all phenomena it still provides a valid estimate of the shoreline wave parameters.

Currently, as there are no available datasets within the model domain, the spatial validation of the model result is unavailable. Due to the location of the AWAC and its proximity to the proposed WEC development sites the spatial degradation of the accuracy of the result is assumed to be minimal; however the level of uncertainty surrounding the accuracy of the result increases with distance away from the temporally calibrated AWAC position. Further work on quantifying the available wave resource for the west coast of Lewis is on-going.

This will include the comparison of modelled and measured wave spectra at the AWAC location, reassessing the spatial wave energy distribution using depth dependent parameters, and using the shoreline distribution results to identify possible future sites based on current WEC technologies.

Future research could also cover the development of a calibration procedure that utilizes directional frequency spectra to calibrate wave models. This process will include large amounts of data for each model time step resulting in a more accurate model.

5. CONCLUSIONS

A calibrated and validated numerical wave model using Mike21 spectral wave module has been developed and applied to the Outer Hebrides for the purpose of simulating nearshore wave spectra and other wave parameters relevant to wave energy application. The model result shows a good agreement with the measured data from the Acoustic Wave and Current profiler (AWAC), showing a wave height scatter index of 0.13 and mean wave period scatter index of 0.14. The peak wave period scatter index was calculated at 0.07. The agreement of the peak wave period value is expected to be lower than the mean wave period due to the high occurrence of dominant long period swell waves. This model provides a good representation of all wave parameters for the location of the AWAC. The variations observed within the wave period dimensions could be attributed to slight evolution of the wave spectra caused by local wind. More data which can be added to the model and may increase model accuracy includes the local effects of wind across the model domain.

The spatial distribution of wave power across the area of interest sees a general increase in power in deeper waters. When shallow water shore regions are considered increased wave power can be seen around exposed outcrops while lower power areas tend to be located in sheltered inlets. When the proposed WEC array sites of Siadar 1 and 2 are compared, the surrounding bathymetric variation causes the focusing of waves towards site 2 resulting in a higher average wave power. The distribution of resource at the 10m contour shows the average power at site 1 and 2 as 25.03kW/m and 28.96kW/m respectively. Additional data presented within this study quantifies and presents the average distribution of wave power across the 10m contour on the north-west coast of the Isle of Lewis.

ACKNOWLEDGMENTS

The authors wish to acknowledge the funding received from the European Regional Development Fund and the primarily SFC funded Hebridean Marine Energy Futures Project. Furthermore the author is grateful for the data and support from the Hebridean Marine Energy Futures project partners Aquamarine Power and Voith Hydro Wavegen and Lews Castle College.

Copyright © 2013 by ASME

REFERENCES

[1] Scottish Government (2011) "2020 Route Map for Renewable Energy in Scotland,"

[2]Aquamarine Power, www.aquamarinepower.com

[3]Pelamis Wave Power, www.pelamiswave.com

[4]Voith Hydro Wavegen, www.wavegen.co.uk

[5] Danish Hydraulic Institute, (2011) "MIKE 21 Spectral Waves FM – Short Description," Hørsholm, Denmark.

[6] Department of Business Enterprise and Regulatory Reform (BERR) (2008) "Atlas of UK Marine Renewable Energy Resource," www.renewables-atlas.info/downloads/documents/Renewable_Atlas_Pages_A4_April08.pdf.

[7] The Crown Estate (2012) "UK Wave and Tidal Key Resource Areas Project Summary Report," www.thecrownestate.co.uk/media/355255/uk-wave-and-tidal-key-resource-areas-project.pdf.

[8]Carbon Trust (2012) "UK Wave Energy Resource," www.carbontrust.com/media/202649/ctc816-uk-wave-energy-resource.pdf.

[9] Venugopal, V. Smith, G,H. (2007) "Wave Climate Investigation for an Array of Wave Power Devices" Proc. 7th European Wave and Tidal Energy Conference, Porto, Portugal

[10] Smith, H,C,M. Pearce, C. Millar, D,L. (2012) "Further Analysis of Changes in Nearshore Wave Climate: An enhanced case study for the Wave Hub site," Renewable Energy, 40, pp.51-64.

[11] The General Bathymetric Charts of the Oceans (GEBCO), www.gebco.net.

[12] Datawell "Datawell conventions for coordinate systems, angles, directions, Fourier transformations and other minus-signs,"

[13] Hasselmann, K.(1974) "On The Spectral Dissipation of Ocean Wave due to White Capping," Boundary Layer Meteorology, 6(1-2), pp. 107-127.

[14] Battjes, J, A., Janssen, J,P,F,M., (1978) "Energy loss and set-up due to Breaking of Random Waves," Proc. 16th International Conference on Coastal Engineering, pp. 569-587.

[15] Ris, R, C. Holthuijsen, H. Booij. N. (1999) "A third-generation wave model for coastal regions, Part 2 Verification" Journal of Geophysical Research, 104, pp.7667-7681.

Copyright © 2013 by ASME